*Int. J. Solids Structures* Vol. 25, No. 1, pp. 45–66, 1989
Printed in Great Britain.

0020-7683/89 $3.00 + .00


# TIME EVOLUTION OF OVERSTRESS PROFILES NEAR BROKEN FIBERS IN A COMPOSITE WITH A VISCOELASTIC MATRIX

DIMITRIS C. LAGOUDAS†
Mathematical Sciences Institute, Cornell University, Ithaca, NY 14853, U.S.A.

CHUNG-YUEN HUI
Theoretical and Applied Mechanics, Cornell University, Ithaca, NY 14853, U.S.A.

and

S. LEIGH PHOENIX
Sibley School of Mechanical and Aerospace Engineering, Cornell University, Ithaca, NY 14853, U.S.A.

(*Received* 11 *September* 1987; *in revised form* 16 *May* 1988)

**Abstract** – The shear-lag model is applied to a monolayer, unidirectional, fiber-reinforced composite loaded in tension. The monolayer contains an infinite number of parallel fibers, with an arbitrary number of them broken simultaneously. While the fibers are modeled as linear elastic, a linear viscoelastic constitutive law is assumed for the matrix material. The time evolution of the overstress profiles in the fibers and matrix near breaks is determined and the time dependence of the effective load transfer length is calculated. Exact closed-form solutions as well as approximate evaluations of the above quantities are given for a power-law creep compliance model, suitable for most epoxy thermosetting resins as matrix materials. These results are also extended to the case of sequential breaks in time and the case of an idealized indentation test.

## 1. INTRODUCTION

The shear-lag model for a unidirectional composite was developed by Hedgepeth (1961) as an attempt to describe the stress fields near broken fibers. It is a simplified micromechanics model for which closed-form solutions can be obtained. In Hedgepeth's analysis an array of parallel, equally spaced fibers of infinite length, forming a monolayer is considered. The monolayer includes an infinite number of fibers with a cluster of them broken (Fig. 1) and is loaded by uniformly distributed tensile tractions in the direction of the fibers. Both fiber and matrix materials are assumed to be linear elastic. The simplification introduced by the shear-lag model is the decoupling between the mechanisms that respond to shear and normal stresses in the composite. It is thus assumed that the fibers alone bear the normal stresses along the fiber direction, while the matrix material acts only as a shear transfer mechanism that overloads the adjacent fibers in tension whenever a fiber breaks.

The influence function technique was used for the solution of the above problem and the explicit evaluation of the overload coefficients of the intact fibers due to fiber breaks was given by Hedgepeth (1961). Closed-form solutions in terms of Bessel and Weber functions for the overload and displacement fields of the fibers were reported by Fichter (1969, 1970), who also looked into the problem of more than one group of breaks. A later work by Hedgepeth and Van Dyke (1967) incorporated an elastic perfectly plastic model for the matrix material. In a subsequent work Van Dyke and Hedgepeth (1969) assumed that the matrix fails completely when a maximum shear stress is reached. A modified version of Hedgepeth's shear-lag analysis was undertaken by Eringen and Kim (1974), who took into account the normal stresses in the matrix transversely to the direction of the fibers. Along the same lines was the analysis of Goree and Gross (1979) with the additional

† Present address: Department of Civil Engineering, Rensellaer Polytechnic Institute, Troy, NY 12180, U.S.A.

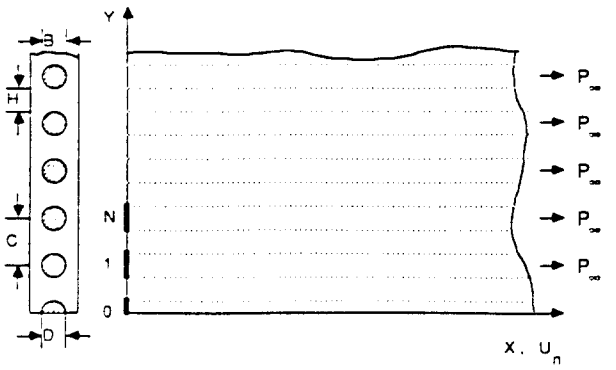


Fig. 1. A unidirectional composite with an infinite number of parallel fibers loaded in tension uniformly, with $(2N+1)$ broken fibers along the $Y$-axis.

inclusion of longitudinal yielding and splitting of the matrix and later on an extension to the three-dimensional case (Goree and Gross, 1980). Comparisons of the predictions of the shear-lag model with three-dimensional finite element calculations were done by Reedy (1984). He found excellent agreement between the two methods for the fiber stress concentrations in a Kevlar epoxy monolayer for load levels that do not cause matrix yielding.

In the present work we analyze the time response predicted by the shear-lag model of a unidirectional, monolayer composite with an infinite number of parallel fibers loaded in tension in the direction of the fibers, by assuming a time-dependent constitutive model for the matrix material. We take the matrix to be linear viscoelastic, and as a special case we investigate the consequences of a power-law, time-dependent, creep compliance on the time evolution of the overstress profiles around broken fibers. Such a power-law creep compliance is commonly used to model the time response of epoxy thermosetting resins, which are often used as the matrix material for non-metallic composites (Pomeroy, 1978). A linear viscoelastic model for the matrix has previously been used by Lifshitz and Rotem (1970) in their statistical theory of failure for composites, where Schapery's approximate technique was used to obtain the time-dependent solution of a shear-lag model that lumped all broken fibers into a single broken fiber.

In Section 2 the formulation and the method of solution of the shear-lag problem is presented for a unidirectional composite under tension with broken elastic fibers and viscoelastic matrix. In Section 3 the time evolution of overstress profiles in the intact fibers, the shear stresses in the matrix and the effective load transfer length are explicitly presented for a matrix that has a power-law creep compliance. Approximate transform inversions and some asymptotic results are given in Section 4. A brief discussion of the case of sequential breaks in time is pursued in Section 5. In Section 6 we apply the shear-lag model to analyze the stress relaxation in an indentation experiment. In these experiments the indentor imposes constant displacement boundary conditions on the broken fiber, while the loads in the intact fibers relax with time as a result of the viscoelastic properties of the matrix.

## 2. FORMULATION OF THE SHEAR-LAG PROBLEM

The model of a unidirectional lamina is shown in Fig. 1, where all fibers are identical and parallel to the $X$-axis and have an equal center-line spacing. The lamina is considered to be a two-dimensional infinite region with an infinite number of fibers, out of which $(2N+1)$ neighboring fibers are broken along the $Y$-axis. In a real case the size of the lamina is finite, but the diameter of the fibers $D$, as well as the fiber spacing are small compared to the length of the fibers. Both the $X$- and $Y$-axes are axes of symmetry for the lamina in terms of geometry and loading and for this reason only one quarter of the lamina is shown in Fig. 1. The external loading is uniform tension applied in the direction of the fibers, which are assumed to be the only tensile load bearing members. This is a justifiable assumption for most polymeric matrix composites because the Young's modulus of the

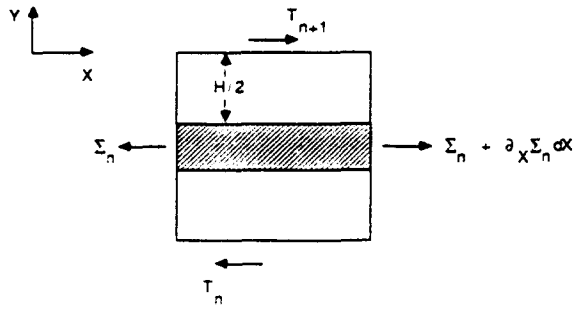


Fig. 2. Equilibrium in the $X$-direction of an infinitesimal element of the $n$th fiber with its surrounding matrix.

matrix is usually one or more orders of magnitude less than the axial Young's modulus of the fibers.

The mechanism of the shear-lag model is a highly idealized one. At zero time the fibers are under constant tensile stress $4P_x/\pi D^2$ along the fiber direction and the matrix material is assumed to be completely relaxed. At time $T = 0^+$, $(2N+1)$ fibers are broken causing overloading of the intact fibers through shear stress in the matrix. The overload region grows with time as a result of the viscoelastic properties of the matrix. We are interested in calculating the time evolution of the stress fields near the breaks in the fibers and the matrix.

A free body diagram, indicating equilibrium of forces in the $X$-direction, of an infinitesimal portion of the $n$th fiber together with its surrounding matrix is shown in Fig. 2 under the shear-lag approximation. By $\Sigma_n$ we denote the mean value of the normal stress $\sigma_{XX}$ along the fiber direction averaged over its cross-section, while $T_n$ and $T_{n+1}$ are the mean values of the shear stresses $\sigma_{YX}$ in the matrix averaged over the *effective thickness* of the lamina $B$. The effective thickness is usually taken to be equal to the diameter of the fibers, namely $B \cong D$. Detailed discussion on the selection of $B$ is given by Reedy (1984). Following his suggestion, we also take the *shear transfer width* $H$ to be given by $H \cong C - \pi D/4$, where $C$ is the fiber spacing, so that the cross-section, $A$, of the fibers remains $\pi D^2/4$. If we neglect inertial forces, equilibrium of forces in the $X$-direction reduces to

$$A\frac{\partial \Sigma_n}{\partial X} + B(T_{n+1} - T_n) = 0, \quad \forall n. \tag{1}$$

The above equations imply that the variation of the normal load $P_n \equiv A\Sigma_n$ transfered along a fiber is equilibrated by the difference in the shear stresses applied by the matrix on both sides of the fiber. Note that $\Sigma_n$ is much larger than $T_{n+1}$, $T_n$ and the normal stresses in the matrix, for a typical polymeric matrix composite. The derivative of $\Sigma_n$ with respect to $X$, however, is of the same order as the shear stress in the matrix, and this is what eqn (1) implies. We have also neglected the derivative with respect to $X$ of the mean value of the normal stress $\sigma_{XX}$ in the matrix because it is much smaller than both terms in eqn (1), even though the mean normal stress itself is of the same order as $T_n$.

Upon specifying constitutive relations for the matrix and fibers, the above set of equations becomes a system of differential-difference equations for the determination of the displacement fields $U_n$ of the cross-sections of the fibers along their axes, as functions of position $X$ and time $T$. In the present work we assume that the fibers are linear elastic, namely

$$P_n(X, T) = AE\frac{\partial U_n(X, T)}{\partial X} \tag{2}$$

where $E$ is the axial Young's modulus of the fibers and $U_n$ the displacement in the $X$-direction of the $n$th fiber. The matrix material is taken to be linear viscoelastic in shear, that is

$$T_n(X,T) = \int_{-\infty}^{T} G(T-S)\frac{\partial \gamma_n(X,S)}{\partial S}\,dS \tag{3}$$

where $G(T)$ is the relaxation modulus and $\gamma_n(X,T)$ the shear strain in the matrix and is approximated by

$$\gamma_n \cong (U_n - U_{n-1})/H. \tag{4}$$

Equation (4) can also be obtained by neglecting the term $\partial_Y(V_{n-1}+V_n)/2$ in the work of Eringen and Kim (1974), where $V_n$ is the displacement in the $Y$-direction of the $n$th fiber. Substitution of eqn (4) into eqn (3) results in

$$T_n(X,T) = \frac{1}{H}\left[\int_{-\infty}^{T} G(T-S)\frac{\partial U_n(X,S)}{\partial S}\,dS - \int_{-\infty}^{T} G(T-S)\frac{\partial U_{n-1}(X,S)}{\partial S}\,dS\right]. \tag{5}$$

We nondimensionalize the time variable by dividing $T$ by some characteristic time $T_c$ of the matrix material, to be found by creep experiments, so that $t \equiv T/T_c$. We also define a normalized relaxation modulus $\mathcal{G}(t) \equiv G(tT_c)/G_e$, where $G_e$ is the instantaneous elastic shear modulus of the matrix material. (In this work lower case letters and script letters denote dimensionless quantities, while upper case letters stand for dimensional quantities.) Substitution of eqns (2) and (5) into eqn (1), yields second-order differential-difference equations for the determination of $U_n$, namely

$$\frac{AEH}{G_e B}\frac{\partial^2 U_n}{\partial X^2} + \int_{-\infty}^{t} \mathcal{G}(t-\zeta)\frac{\partial}{\partial \zeta}(U_{n+1} - 2U_n + U_{n-1})\,d\zeta = 0, \quad \forall n. \tag{6}$$

If the solution of eqn (6) is found, substitution of $U_n$ into eqn (5) will yield the shear stress in the matrix $T_n$ and substitution into eqn (2) will yield the normal loads in the fibers. $X$ and $U_n$ are normalized so that the field equations and the boundary and initial conditions become independent of the material parameters. By defining $x \equiv X/X_c \equiv X/\sqrt{(AEH/G_eB)}$ and $u_n(x,t) \equiv U_n(X,T)/\sqrt{(P_z^2 H/G_e AEB)}$, eqn (6) becomes

$$\frac{\partial^2 u_n}{\partial x^2} + \int_{-\infty}^{t} \mathcal{G}(t-\zeta)\frac{\partial}{\partial \zeta}(u_{n+1} - 2u_n + u_{n-1})\,d\zeta = 0, \quad \forall n. \tag{7}$$

The boundary conditions are given by

$$\frac{\partial u_n}{\partial x} = 1, \quad \forall n, \quad x \to \infty, \quad t > 0 \tag{8a}$$

$$\frac{\partial u_n}{\partial x} = 0, \quad |n| \leqslant N, \quad x = 0, \quad t > 0 \tag{8b}$$

$$u_n = 0, \quad |n| > N, \quad x = 0, \quad t > 0 \tag{8c}$$

while the initial conditions are

$$u_n = x, \quad \forall n, \quad x \geqslant 0, \quad t = 0. \tag{9}$$

To avoid unbounded displacement fields in the analysis, the transformation

$$w_n = u_n - x \tag{10}$$

is introduced, which, after its substitution into eqns (7)–(9), results in the following field equations, boundary and initial conditions:

$$\frac{\partial^2 w_n}{\partial x^2} + \int_{-\infty}^{t} \mathscr{G}(t-\zeta) \frac{\partial}{\partial \zeta}(w_{n+1} - 2w_n + w_{n-1})\, \mathrm{d}\zeta = 0, \quad \forall n \tag{11}$$

$$\frac{\partial w_n}{\partial x} = 0, \quad \forall n, \quad x \to \infty, \quad t > 0 \tag{12a}$$

$$\frac{\partial w_n}{\partial x} = -1, \quad |n| \leqslant N, \quad x = 0, \quad t > 0 \tag{12b}$$

$$w_n = 0, \quad |n| > N, \quad x = 0, \quad t > 0 \tag{12c}$$

$$w_n = 0, \quad \forall n, \quad x \geqslant 0, \quad t = 0. \tag{13}$$

Notice that the field equations remain unchanged in form. The change in the boundary conditions has altered the original problem into a new one, in which there are no loads at infinity and there are only compressive loads applied on the broken fibers suddenly at $t = 0^+$, which open up the breaks as $t$ grows.

The above equations can be solved by using the method of Laplace transform. If $\bar{\mathscr{G}}(s)$ and $\bar{w}_n(x,s)$ denote the Laplace transforms of $\mathscr{G}(t)$ and $w_n(x,t)$, respectively, the Laplace transforms of eqns (11) and (12), upon using eqn (13), become

$$\frac{\partial^2 \bar{w}_n(x,s)}{\partial x^2} + s\bar{\mathscr{G}}(s)[\bar{w}_{n+1}(x,s) - 2\bar{w}_n(x,s) + \bar{w}_{n-1}(x,s)] = 0, \quad \forall n \tag{14}$$

$$\frac{\partial \bar{w}_n}{\partial x} = 0, \quad \forall n, \quad x \to \infty \tag{15}$$

$$\frac{\partial \bar{w}_n}{\partial x} = -\frac{1}{s}, \quad |n| \leqslant N, \quad x = 0 \tag{16a}$$

$$\bar{w}_n = 0, \quad |n| > N, \quad x = 0. \tag{16b}$$

We have thus transformed the original viscoelastic problem into an elastic shear-lag problem (correspondence principle, Christensen (1982)). We will follow here the methodology presented by Eringen and Kim (1974) and used also by Goree and Gross (1979) for the solution of the elastic shear-lag problem, which is a dual integral equation technique. However, one can also use the influence function technique developed by Hedgepeth (1961).

We can reduce eqn (14) to a single differential equation by introducing the finite cosine transform (Churchill, 1972), i.e.

$$\bar{w} = \frac{\bar{w}_0}{\pi} + \frac{2}{\pi} \sum_{n=1}^{\infty} \bar{w}_n \cos(n\theta), \quad 0 < \theta < \pi \tag{17a}$$

with the inversion formula given by

$$\bar{w}_n = \int_0^{\pi} \bar{w} \cos(n\theta)\, \mathrm{d}\theta, \quad n \geqslant 0 \tag{17b}$$

where $\bar{w} \equiv \bar{w}(x,s,\theta)$, $\bar{w}_n \equiv \bar{w}_n(x,s)$. By summing eqns (14) with $n$ running from $-\infty$ to

$\infty$, after having multiplied by $\cos(n\theta)$, and by taking into account the symmetry $\bar{w}_n(x,s) = \bar{w}_{-n}(x,s)$, it is found that $\bar{w}$ satisfies

$$\frac{\partial^2 \bar{w}}{\partial x^2} - 4s\bar{\mathcal{G}}(s)\sin^2(\theta/2)\bar{w} = 0. \tag{18}$$

The resulting simplification in the field equations has shifted the difficulty into the boundary conditions, which turn out to be integral equations, namely

$$\frac{\partial \bar{w}}{\partial x} = 0, \quad x \to \infty \tag{19}$$

$$\int_0^{\pi} \frac{\partial \bar{w}}{\partial x}\cos(n\theta)\,\mathrm{d}\theta = -\frac{1}{s}, \quad 0 \leqslant n \leqslant N, \quad x = 0 \tag{20a}$$

$$\int_0^{\pi} \bar{w}\cos(n\theta)\,\mathrm{d}\theta = 0, \quad N < n < \infty, \quad x = 0. \tag{20b}$$

A solution to eqn (18) that satisfies boundary condition (19) is given by

$$\bar{w} = f(s,\theta)\exp\left[-2\sin(\theta/2)x\sqrt{(s\bar{\mathcal{G}}(s))}\right] \tag{21}$$

for some $f(s,\theta)$. Substitution of eqn (21) into eqns (20a) and (20b) yields the conditions

$$\int_0^{\pi} f(s,\theta)\sin(\theta/2)\cos(n\theta)\,\mathrm{d}\theta = \frac{1}{2s\sqrt{(s\bar{\mathcal{G}}(s))}}, \quad 0 \leqslant n \leqslant N \tag{22a}$$

$$\int_0^{\pi} f(s,\theta)\cos(n\theta)\,\mathrm{d}\theta = 0, \quad N < n < \infty \tag{22b}$$

for $f(s,\theta)$. If we let

$$f(s,\theta) \equiv \sum_{m=0}^{N} b_m \cos(m\theta)/\left[2s\sqrt{(s\bar{\mathcal{G}}(s))}\right]$$

conditions (22a) for the broken fibers reduce to

$$\sum_{m=0}^{N} b_m \int_0^{\pi} \sin(\theta/2)\cos(n\theta)\cos(m\theta)\,\mathrm{d}\theta = 1, \quad 0 \leqslant n \leqslant N \tag{23}$$

while conditions (22b) for the intact fibers are satisfied identically. The complete satisfaction of the boundary conditions reduces then to the solution of the algebraic system (23) of $(N+1)$ equations, for the determination of the $(N+1)$ unknown coefficients $b_m$, $m = 0, 1, 2, \ldots, N$. The solution to the transformed problem is found by substituting $\bar{w}$ from eqn (21) into eqn (17b) and is given by the following expression:

$$\bar{w}_n(x,s) = \sum_{m=0}^{N} \frac{b_m}{2s\sqrt{(s\bar{\mathcal{G}}(s))}} \int_0^{\pi} \exp\left[-2\sin(\theta/2)\sqrt{(s\bar{\mathcal{G}}(s))}x\right]\cos(m\theta)\cos(n\theta)\,\mathrm{d}\theta. \tag{24}$$

The inversion of the Laplace transforms of $\bar{w}_n$ will result in $w_n(x,t)$. The difficulty of the inversion will mainly depend on the selection of the constitutive model (i.e. $\bar{\mathcal{G}}(s)$) for the viscoelastic matrix.

A clarifying remark regarding the number of broken fibers is mentioned at this point. We have assumed that the number of breaks is an odd integer, namely $(2N+1)$, and as a

consequence we have used the finite cosine transform (17), taking into account the symmetry of $\bar{w}_n(\bar{w}_n = \bar{w}_{-n})$. We could easily model any number of breaks by using the finite exponential transform (Churchill, 1972), which reduces to the finite cosine transform whenever $\bar{w}_n = \bar{w}_{-n}$. The only change in the previous analysis is that $f(s, \theta)$ is now given by

$$\sum_{m=-M}^{N} b_m/[2s\sqrt{(s\bar{\mathcal{G}}(s))}] \exp(-im\theta),$$

where the total number of breaks is $(M+N+1)$ and the algebraic system (23) involves $(M+N+1)$ unknown coefficients $b_m$.

The important quantities in the analysis of shear-lag models are the overloads in the fibers near breaks and the shear stresses in the matrix. The non-dimensional loads in the fibers, defined by $p_n(x, t) \equiv P_n(xX_c, tT_c)/P_\infty$, can be found by substituting $w_n(x, t)$ from eqn (24) into eqn (2) upon using eqn (10), and they are given by

$$p_n(x, t) = \frac{\partial w_n(x, t)}{\partial x} + 1, \quad n \geq 0. \tag{25}$$

The normalized shear stresses $\tau_n(x, t) \equiv T_n(xX_c, tT_c)/\sqrt{(P_\infty^2 G_c/AEBH)}$ between the $n$th and the $(n-1)$th fibers are evaluated by substitution of $w_n(x, t)$ into eqn (5) (which upon using eqn (10) yields the normalization), and they are given by

$$\tau_n(x, t) = \int_0^t \mathcal{G}(\tau - \zeta) \frac{\partial(w_n - w_{n-1})}{\partial \zeta} \, d\zeta, \quad n \geq 1. \tag{26}$$

Another useful quantity, especially for statistical models of failure of composites (Phoenix *et al.*, 1988), is the *effective load transfer length* $L_f$, which for the present purposes is defined as the distance from the breaks in the $x$-direction, within which the *overload* $(p_{N+1} - 1)$ of the first unbroken fiber has dropped to zero. Since in the shear-lag model the load $P_{N+1}$ of the first intact fiber actually descends to values below $P_\infty$ before it decays exponentially to $P_\infty$ as $x \to \infty$, we define $L_f$ as the distance from the breaks at which $P_{N+1}$ crosses $P_\infty$. In this case $L_f$ or equivalently the normalized effective load transfer length $l_f \equiv L_f/\sqrt{(AEH/G_c B)}$ must satisfy the conditions

$$p_{N+1}(l_f, t) = 1 \quad \text{or} \quad \frac{\partial w_{N+1}(l_f, t)}{\partial x} = 0. \tag{27}$$

In general $l_f$ will depend on time because $p_{N+1}$ depends on time. The so defined $l_f$ becomes a characteristic length for the whole laminate for a given number of breaks $(2N+1)$.

We summarize the results of this section by giving explicit evaluations for the quantities of interest. The number of broken fibers $(2N+1)$ is assumed to be known, while the constants $b_m$ are obtained by solving the linear algebraic system of eqns (23). The fiber cross-section displacements, fiber axial loads and shear stresses in the matrix are then calculated by using eqns (24)–(26), respectively. These equations acquire the following explicit evaluations:

$$w_n(x, t) = \sum_{m=0}^{N} b_m \int_0^\pi L^{-1}\{\exp[-2 \sin(\theta/2)\sqrt{(s\bar{\mathcal{G}}(s))}x]/(2s\sqrt{(s\bar{\mathcal{G}}(s))})\} \cdot \cos(m\theta) \cos(n\theta) \, d\theta \tag{28}$$

$$p_n(x, t) = 1 - \sum_{m=0}^{N} b_m \int_0^\pi L^{-1}\{\exp[-2 \sin(\theta/2)\sqrt{(s\bar{\mathcal{G}}(s))}x]/s\} \cdot \sin(\theta/2) \cos(m\theta) \cos(n\theta) \, d\theta \tag{29}$$

$$\tau_n(x,t) = \sum_{m=0}^{N} b_m \int_0^{\pi} L^{-1}\{\exp[-2\sin(\theta/2)\sqrt{(s\bar{\mathscr{G}}(s))}x]\sqrt{(s\bar{\mathscr{G}}(s))}\,2s\}$$

$$\cdot\cos(m\theta)[\cos(n\theta)-\cos((n-1)\theta)]\,d\theta \quad (30)$$

where

$$f(t) = L^{-1}[\bar{f}(s)] \equiv \frac{1}{2\pi i}\lim_{\beta\to\infty}\int_{\gamma-i\beta}^{\gamma+i\beta}\exp(ts)\bar{f}(s)\,ds, \quad t>0. \quad (31)$$

## 3. POWER-LAW CREEP COMPLIANCE MODEL FOR THE MATRIX MATERIAL

A model that describes closely the viscoelastic properties of commercially used matrix materials (epoxy thermosetting resins) is a power-law creep compliance model, where the creep compliance is given by

$$J(T) = J_c\left[1+\left(\frac{T}{T_c}\right)^{\alpha}\right] = J_c(1+t^{\alpha}) \equiv J_c\mathscr{J}(t). \quad (32)$$

In the above $J_c$ denotes the instantaneous elastic compliance in shear of the matrix material and $T_c$ and $\alpha$ are material constants. $T_c$ is the characteristic time required for the initial displacement to be doubled, while the exponent $\alpha$ is usually much smaller than unity. The limit $\alpha \to 0$ corresponds to the elastic case, while $\alpha \to 1$ gives the Maxwell viscoelastic model. The connection between the relaxation modulus $\mathscr{G}(t)$ and the creep compliance $\mathscr{J}(t)$ is expressed through the Laplace transformed quantities (Christensen, 1982) by

$$\bar{\mathscr{G}}(s)\,\bar{\mathscr{J}}(s)s^2 = 1 \quad (33)$$

if $G_c = 1/J_c$. From eqns (32) and (33) the Laplace transform of the relaxation modulus is found to be

$$s\bar{\mathscr{G}}(s) = \frac{s^{\alpha}}{s^{\alpha}+\Gamma(\alpha+1)}. \quad (34)$$

By inserting eqns (34) into eqns (28)–(30) it is possible to obtain explicit evaluations for $w_n$, $p_n$ and $\tau_n$ in terms of $x$ and $t$ for different values of $\alpha$. The inversion of the Laplace transforms has been obtained by contour integration. We will only report here the solution for the fiber loads and the shear stresses, while the displacement fields can be obtained by integrating eqn (25). The fiber loads and the shear stresses are found to be

$$p_n(x,t) = 1 - \sum_{m=0}^{N} b_m \int_0^{\pi} h(x,t,\theta)\cos(m\theta)\cos(n\theta)\sin(\theta/2)\,d\theta \quad (35)$$

$$\tau_n(x,t) = \sum_{m=0}^{N} b_m \int_0^{\pi} g(x,t,\theta)\cos(m\theta)[\cos(n\theta)-\cos((n-1)\theta)]\,d\theta \quad (36)$$

where the functions $h(x,t,\theta)$ and $g(x,t,\theta)$ are given in Appendix A.

Numerical integration of the above formulae has been carried out for both $p_n$ and $\tau_n$, even though they are related through eqn (1). The reason for this is that $p_n$ is usually the quantity of primary interest and the numerical evaluation of $\tau_n$ from $p_n$ involves differentiation which should be avoided. Numerical integration has been done by using a midpoint Romberg integration technique, with an appropriate change of variables at the singular

points of the integrands. The results are plotted in Figs 3–6, for one and three broken fibers and for the first and second intact fibers for various times ($\alpha = 0.1$ for all cases). The elastic solution of Hedgepeth (1961) corresponds effectively to time $t_1$.

From Figs 3 and 4 we notice that at $x = 0$ we recover the overload coefficients ($P_n(x = 0, t)$ $P_x \equiv p_n(x = 0, t)$) in accordance with the elastic solution of Hedgepeth. The overload coefficient of the first intact fiber in a lamina with $(2N+1)$ neighboring breaks as calculated by Hedgepeth is given by

$$\kappa_N = \frac{4 \cdot 6 \cdot 8 \cdot \ldots \cdot (2N+4)}{3 \cdot 5 \cdot 7 \cdot \ldots \cdot (2N+3)}, \quad 0 \leqslant N < \infty. \tag{37}$$

The above formula holds for the viscoelastic case as well because the overall static equilibrium of the composite is not affected by the viscoelastic properties of the matrix material. This is a consequence of the assumption that the matrix material cannot sustain normal loads in the $x$-direction and there is no stress relaxation in the fibers as they are assumed to be elastic. Therefore, the excess load caused by the simultaneous breaks has to be shared by the neighboring intact fibers and only the stress distributions are affected by the viscoelastic properties of the matrix material.

Several observations can be drawn from Figs 3 and 4. The slope of the load distribution in the fibers decreases in absolute value as time increases, resulting in a growth of the effective load transfer length $l_t$ with time (Figs 3(a) and 4(a)). The overload $[p_n(x, t) - 1]$ undershoots and actually becomes negative before it decays to zero as $x \to \infty$ for the intact fibers. Global equilibrium of the composite in the $x$-direction implies that $\sum_i [p_n(x, t) - 1] = 0$, with summation extending to all fibers. Since the negative overloads in the broken fibers grow with time as a result of the shear stress relaxation in the matrix, the positive overloads in the intact fibers increase with time for fixed $x$, so that global equilibrium is satisfied (Figs 3 and 4). This implies that the probability of failure for the intact fibers near breaks increases with time (Phoenix *et al.*, 1988). The length over which this increased probability occurs also grows with time, this being the effective load transfer length $l_t$.

The relaxation of the shear stress in the matrix can be seen in Figs 5 and 6. The shear-lag model predicts that the maximum shear stress occurs at the break points (Figs 5(a) and 6(a)). It is often believed, using symmetry arguments, that the shear stresses in the matrix should approach zero at the fiber breaks, but as pointed out by others (Goree and Gross, 1980) these stresses need not approach zero at all. Nevertheless, the shear-lag model cannot predict accurately the shear stresses in the immediate vicinity of the breaks. The main reason is that high stress concentrations due to the presence of the crack formed by the broken fibers will lead to debonding and relative slip of points in the fiber–matrix interface. Note, however, that since the fibers are much stiffer than the matrix ($\cong 100$), the region in which the stresses are perturbed due to fiber breaks is 50 or more fiber diameters, while the shear-lag analysis might fail to predict correctly the stresses in a small region of one or two fiber diameters away from the breaks. Even though it is an approximate model, the shear-lag model for the viscoelastic case unravels the trend in the time dependence of the stress fields near broken fibers.

## 4. ASYMPTOTIC EXPANSIONS AND APPROXIMATIONS

The results of the previous section demonstrate the time evolution of the overload zones and the shear stress relaxation. They cannot be readily used for engineering purposes though, because of the complicated form of the solution. We can simplify the results by inverting the Laplace transforms approximately. Approximate inversion techniques have been employed by Schapery (1962) for viscoelastic stress analysis. Such an approximate inversion is derived in Appendix B. Schapery (1967) found that accurate results can be obtained using the approximation theory as long as $\alpha$ is small, which is the case in our

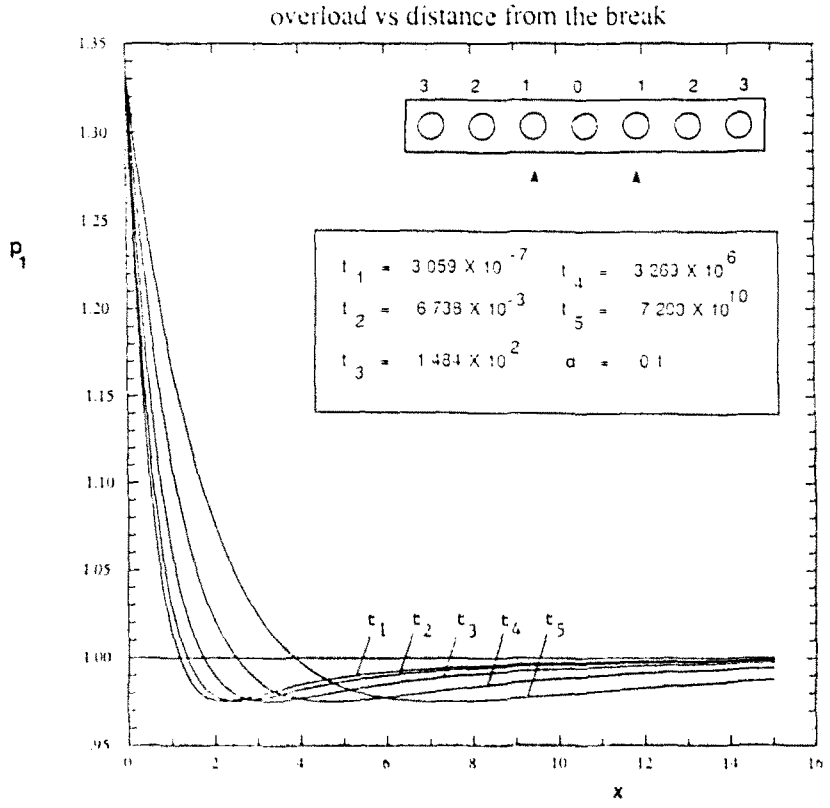


Fig. 3(a). Load profile of the first (adjacent) intact fiber at various times; one break.

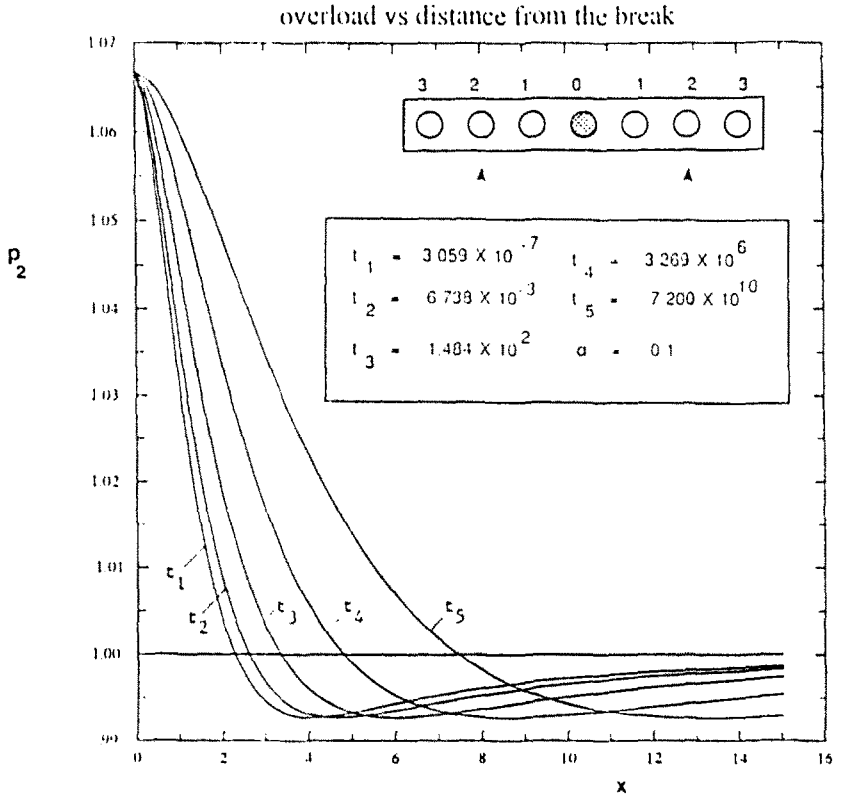


Fig. 3(b). Load profile of the second intact fiber at various times; one break.

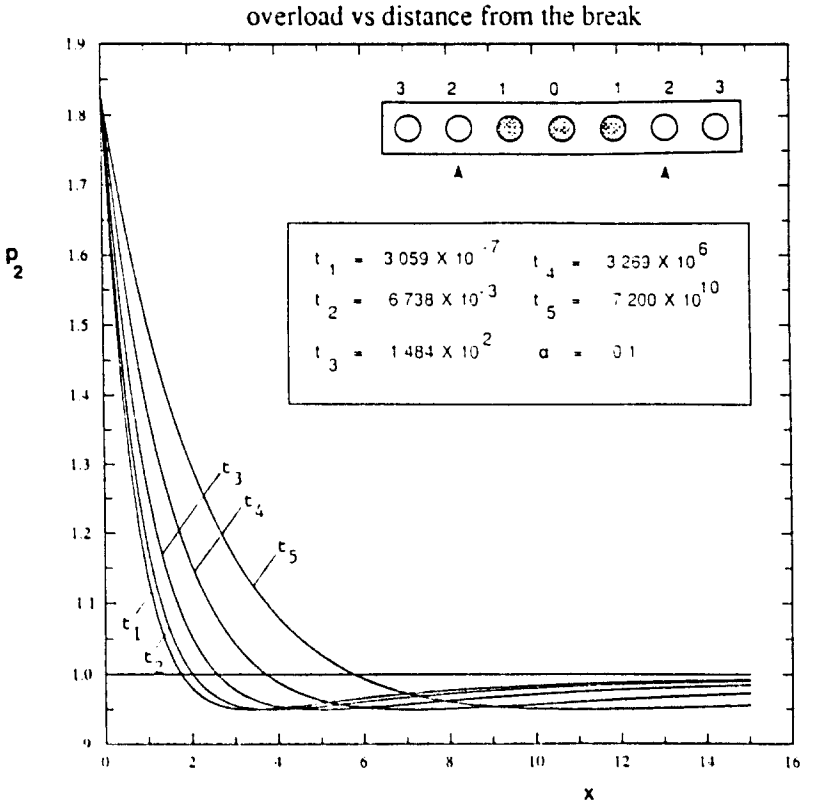


Fig. 4(a). Load profile of the first intact fiber for various times; three breaks.

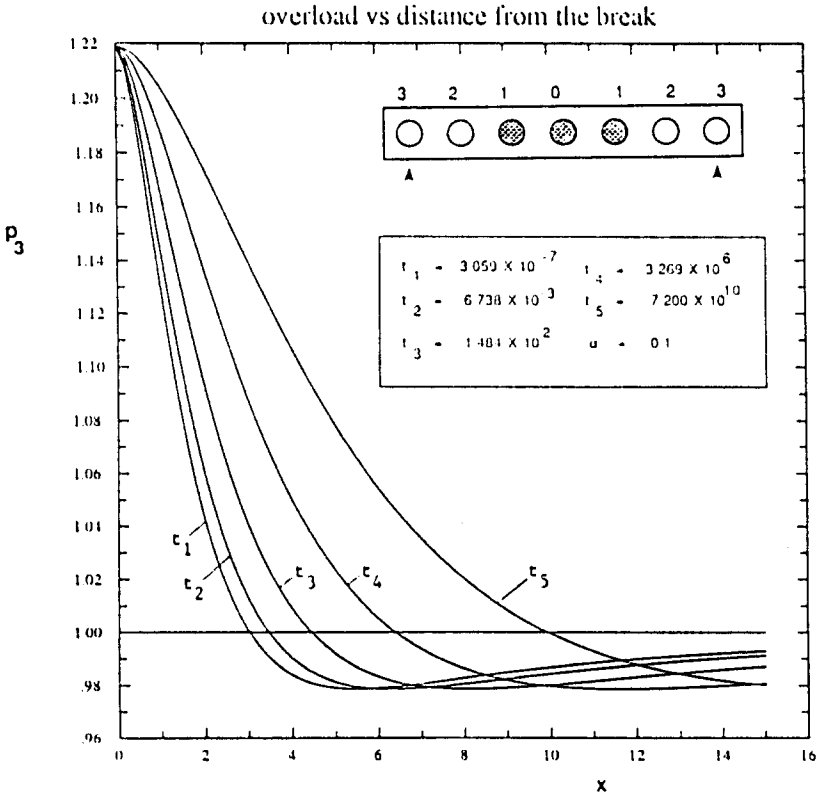


Fig. 4(b). Load profile of the second intact fiber for various times; three breaks.

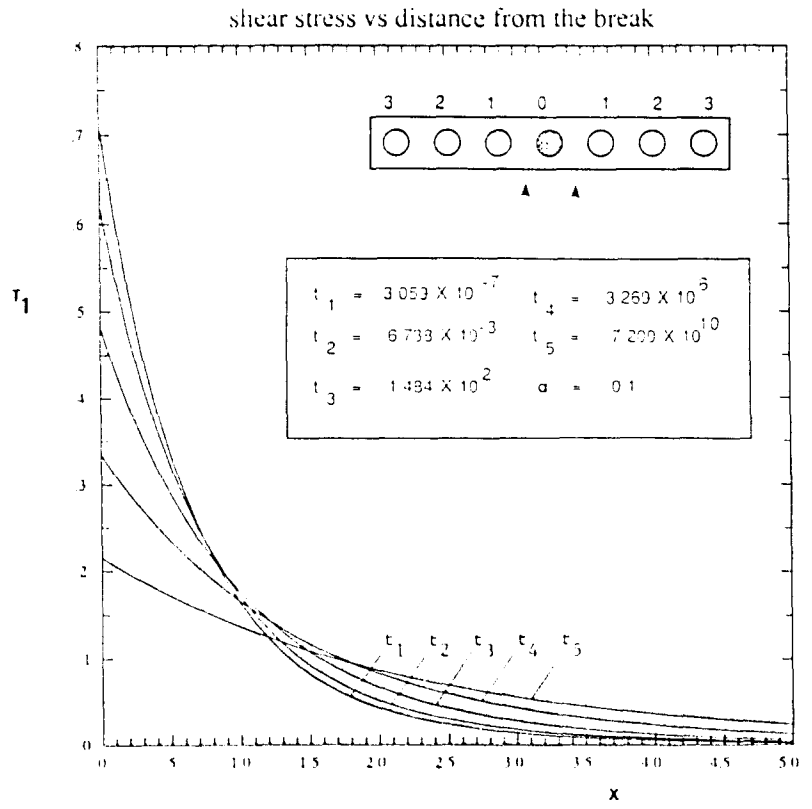


Fig. 5(a). Shear stress in matrix between the broken and the first unbroken fibers for various times; one break.

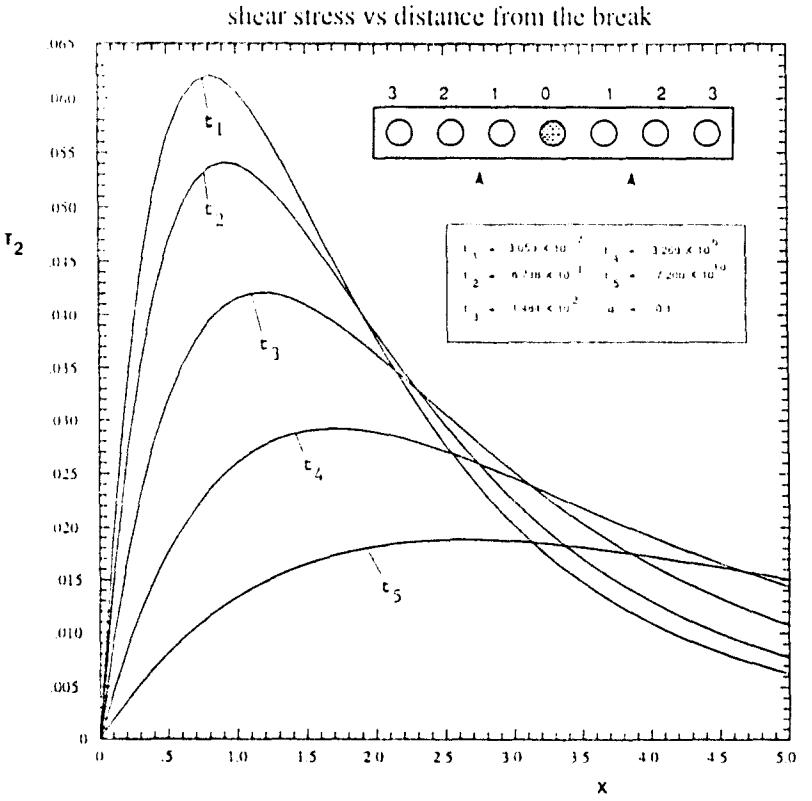


Fig. 5(b). Shear stress in matrix between the first and second intact fibers for various times; one break.

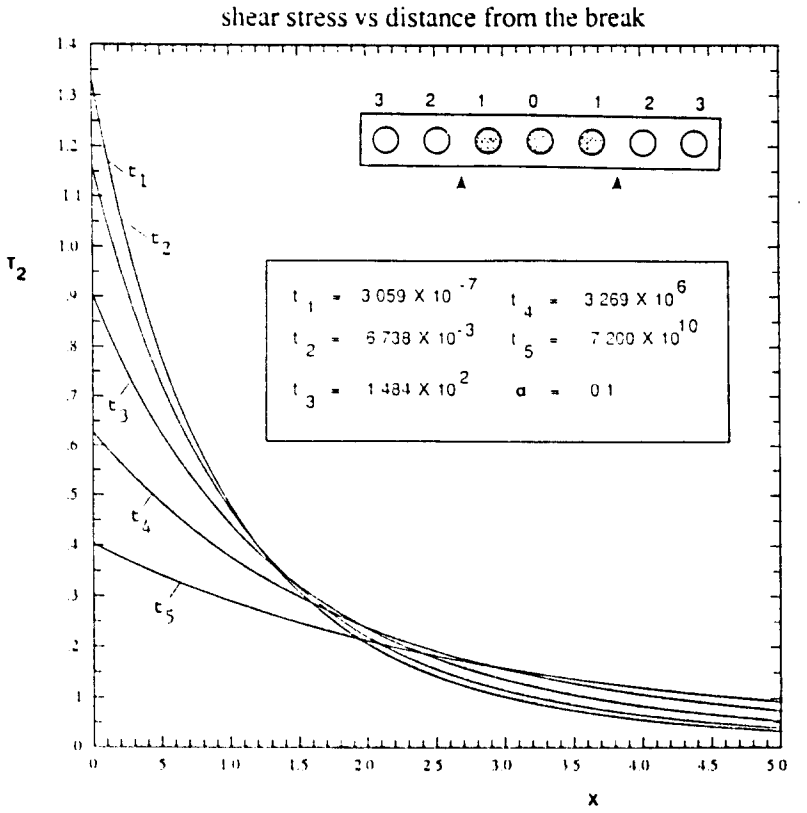


Fig. 6(a). Shear stress in matrix between the last broken and the first unbroken fibers for various times; three breaks.

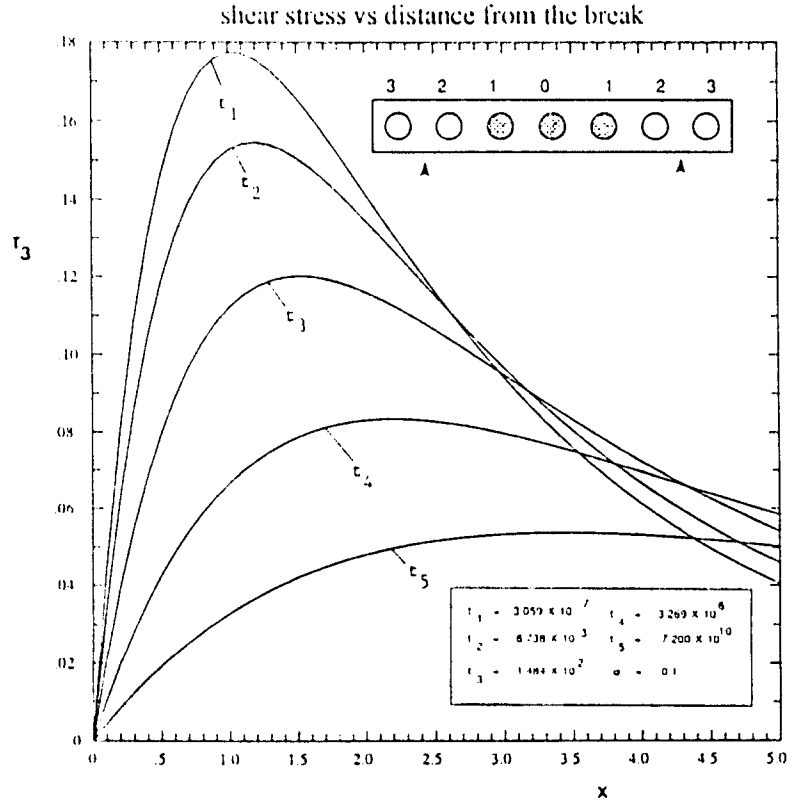


Fig. 6(b). Shear stress in matrix between the first and the second intact fibers for various times; three breaks.

study. It has been found that whenever $\alpha \leqslant 0.1$ the error in the overloads along the fibers does not exceed 1%. Further comparisons with the exact inversion for various $\alpha$ will be given later in this section. Notice that the approximate inversion of the Laplace transforms appearing in eqns (28)–(30) by using eqn (B9) is equivalent to the substitution of the approximate inverse Laplace transform of $\bar{\mathcal{G}}(s)$ into the elastic solution, namely $G_e$ is replaced by $G_e\mathcal{G}(t)$ in the elastic solution, where $\mathcal{G}(t)$ is obtained from $\bar{\mathcal{G}}(s)$ upon using eqn (B9).

The long time behavior of the solution for $p_n(x, t)$ is obtained by applying Watson's lemma (Carrier *et al.*, 1966) to $h(x, t, \theta)$ in eqn (35) and the asymptotic expansion of eqn (35), valid for $t \to \infty$, is given by

$$p_n(x,t) - 1 \cong -d_1(n) + d_2(n)\xi - d_3(n)\xi^2 + d_4(n)\xi^3 - d_5(n)\xi t^{-\alpha} \tag{38}$$

where the functions $d_1(n)$, $d_2(n)$, $d_3(n)$, $d_4(n)$, $d_5(n)$ depend only on the fiber under consideration and $\xi \equiv x/t^{\alpha/2}$ is the similarity variable for large time. Explicit evaluations of these functions are given in Appendix C. A similar result can also be obtained for the shear stress in the matrix by applying Watson's lemma to $g(x, t, \theta)$ in eqn (36). The interesting point here is that the solution for the loads $p_n$ along the fibers is approximately self-similar (the first four terms on the right-hand side of eqn (38)). The plot of $p_n$ vs $\xi$ is approximately a parabola for large values of time and small values of $x$ ($t \to \infty$, $\xi \to 0$). For extremely large times ($\alpha \cong 0.1$) and small $x$ the solution becomes a straight line. For $x = 0$ the overload coefficients for the elastic analysis are recovered, namely $1 - d_1(1) = 4/3$ for one broken fiber, etc. The time variable $t$ enters explicitly into the expression for $p_n$ if terms of order $t^{-3\alpha/2}$ are considered, but for $\xi = O(1)$ the term $d_5(n)\xi t^{-\alpha}$ is negligible for large $t$, and the self-similar character of the solution is not destroyed. This is seen in Fig. 7, where the curves for the overload of the first unbroken fiber for times $t_3$, $t_4$, and $t_5$ almost coincide when we change the abscissa from $x$ to $\xi$.

The asymptotic result for the overloads of the intact fibers can be used to determine the time dependence of the effective load transfer length as defined in Section 2. Upon using eqn (38), the condition $p_{N+1}(l_t, t) = 1$ gives

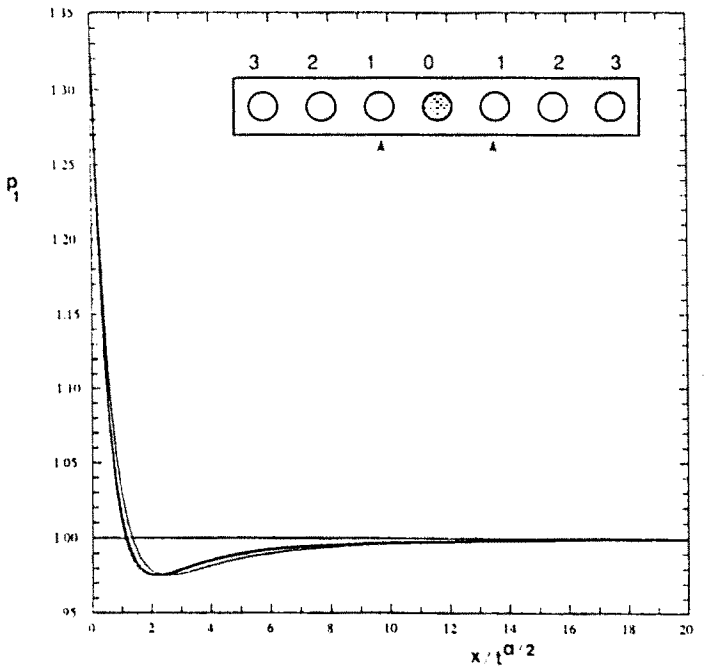


Fig. 7. Load of the first intact fiber as a function of the similarity variable $x/t^{\alpha/2}$ for times $t_3 = 1.484 \times 10^2$, $t_4 = 3.269 \times 10^6$, $t_5 = 7.2 \times 10^{10}$.

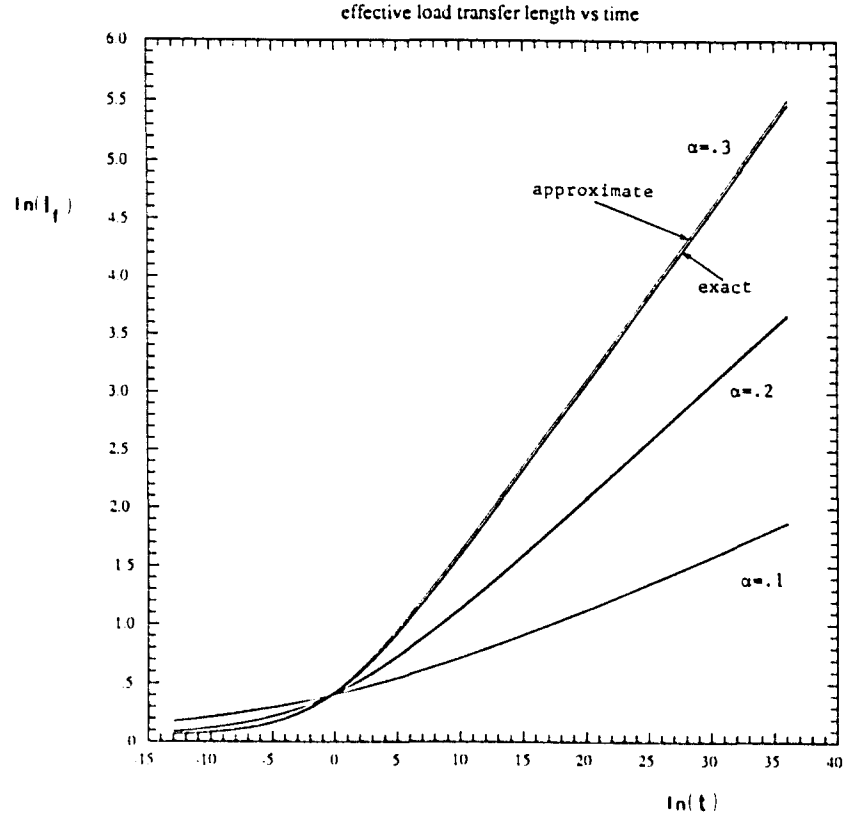


Fig. 8. Effective load transfer length as a function of time for various values of $\alpha$ and for one broken fiber.

$$l_f = z_r t^{\alpha/2} \tag{39}$$

where $z_r$ is the first positive root of the polynomial in $\xi$ on the right-hand side of eqn (38). Note that eqn (38) with only quadratic terms in $\xi$ can be used to evaluate $p_n$ for small values of $\xi$ ($\xi \leqslant 0.5$), otherwise substantial errors are introduced. Since $l_f/t^{\alpha/2}$ is well above 0.5 for most cases, it has been found necessary to include at least cubic terms in the expression for $p_n$. By neglecting the term $d_5(N+1)\xi t^{-\alpha}$, the effective load transfer length becomes proportional to $t^{\alpha/2}$ as $t \to \infty$ with the proportionality constant depending only on $\alpha$ and the number of breaks. The plot in Fig. 8, where $l_f$ is given for both the approximate and the exact Laplace transform inversions, verifies that the power-law time dependence of $l_f$ is a good approximation for large $t$. As $\alpha$ decreases we have to go to higher values in $t$ in order for the power-law to be valid. The curves in Fig. 8 have slope $\alpha/2$ for large values of time and for a given value of $\alpha$ there is a unique curve ln ($l_f$) vs ln ($t$), within a translation along the vertical axis, independent of the number of breaks. For example, the corresponding curves for three broken fibers can be obtained by translating the curves of Fig. 8 (valid for one break) in such a way that at the limit $t \to 0$ the curves predict the elastic $l_f$ for three broken fibers.

The asymptotic behavior of $p_n$ given by eqn (38), which is obtained by using the exact solution for $p_n$ given by eqn (35), is compared with the asymptotic behavior of the approximate solution, which is obtained by using Schapery's approximate method of Laplace inversion (eqn (B9)) and is given by

$$p_n(x,t) \cong 1 - \sum_{m=0}^{N} b_m \int_0^{\pi} \cos(m\theta) \cos(n\theta) \sin(\theta/2)\, d\theta + \frac{2\exp(-\gamma\alpha/2)}{[\Gamma(\alpha+1)]^{1/2}} \frac{x}{t^{\alpha/2}} \sum_{m=0}^{N} b_m \int_0^{\pi} \cos(m\theta) \cos(n\theta) \sin^2(\theta/2)\, d\theta \tag{40}$$

where $\gamma$ is Euler's constant. Expansions (38) and (40) produce identical first-order terms if

$$\exp(-\gamma) = [\Gamma(1-\alpha/2)]^{-2/\alpha}. \tag{41}$$

We indeed observe that $\exp(-\gamma) \cong 0.56$, while $[\Gamma(1-\alpha/2)]^{-2/\alpha}$ ranges between 0.44 and 0.54, for $0.5 < \alpha < 0.1$. Schapery (1962) proposed the use of the value 0.5 instead of $\exp(-\gamma)$ in eqn (B9) because he found that it produces better results for most polymers. In our numerical implementation we have used the value of $[\Gamma(1-\alpha/2)]^{-2/\alpha}$ instead of $\exp(-\gamma)$ for the computation of the effective load transfer length (approximate) reported in Fig. 8. The maximum error in the effective load transfer length is 4.13% for $\alpha = 0.3$, while for smaller values of $\alpha$ the error is negligible (the approximate and the exact $l_f$ coincide for $\alpha = 0.2$ and 0.1 in Fig. 8).

## 5. SEQUENTIAL FIBER-BREAKS

The solution technique presented in Section 2 remains the same for the case when pairwise fiber-breaks occur sequentially in time, triggered by some initial break in the 0th fiber at time $t_0$. The governing equations and boundary and initial conditions for this case are eqns (11)–(13) with the exception of boundary conditions (12b) for the broken fibers, which have to be modified. Let $t_n$, $0 \leqslant n \leqslant N$, denote the time when fibers $n$ and $-n$ break, i.e. $t_0$ is the time of the initial break and $t_N$ the time when the final pair of fibers breaks. The boundary conditions for the $(2N+1)$ broken fibers become

$$\frac{\partial w_n}{\partial x} = q_n^0 H(t-t_0) + (q_n^1 - q_n^0)H(t-t_1) + (q_n^2 - q_n^1)H(t-t_2) + \cdots + (q_n^N - q_n^{N-1})H(t-t_N), \quad x = 0, \quad 0 \leqslant n \leqslant N \tag{42}$$

where $H$ is the Heaviside step function and the constant coefficients $q_n^m$, $0 \leqslant m, n \leqslant N$, are obtained using the normalized overloads predicted by the elastic solution. The superscript $m$ in $q_n^m$ denotes the number of broken pairs of fibers after time $t_m$ ($m$ broken pairs correspond to $(2m+1)$ broken fibers) and before the next pair of breaks occurs. For a fixed $m$ the values of $q_n^m$ are obtained from the relation $q_n^m = p_n(x=0,t) - 1$ as follows.

(a) When the index $n$ corresponds to a broken fiber, namely $0 \leqslant n \leqslant m$, $p_n(0,t) = 0$, whereby $q_n^m = -1$.

(b) When the index $n$ corresponds to a yet intact fiber, namely $m < n \leqslant N$, $p_n(0,t)$ is given by eqn (35), which coincides with the elastic solution of Hedgepeth (1961) at $x = 0$ ($h(0,t,0) = 1$ in eqn (35)). In particular, $q_{m+1}^m = p_{m+1}(0,t) - 1 = \kappa_m - 1$ as given by eqn (37). For example, consider the special case with an initial break at $t = t_0$ and two subsequent breaks at $t_1 > t_0$, so that the total number of broken pairs is $N = 1$. The values of $q_n^m$ are $q_0^0 = -1$, $q_1^0 = 1/3$, $q_0^1 = -1$, $q_1^1 = -1$ (the value of $q_1^0$ can be obtained from eqn (37), i.e. $q_1^0 = p_1(x=0,t) - 1 = \kappa_0 - 1 = 4/3 - 1$) and eqn (42) becomes $\partial w_0/\partial x = -H(t-t_0)$, $\partial w_1/\partial x = 1/3H(t-t_0) - 4/3H(t-t_1)$.

By taking the Laplace transform of eqn (42) and using eqn (24) to evaluate the left-hand side of eqn (42), a system of $(N+1)$ algebraic equations results for the unknown functions $b_m^*(s)$:

$$\sum_{m=0}^{N} c_{nm} b_m^*(s) = -[q_n^0 \exp(-t_0 s) + (q_n^1 - q_n^0)\exp(-t_1 s) + (q_n^2 - q_n^1) \cdot \exp(-t_2 s) + \cdots + (q_n^N - q_n^{N-1})\exp(-t_N s)], \quad 0 \leqslant n \leqslant N \tag{43}$$

where $c_{nm}$ are constants given by

$$c_{nm} = \int_0^\pi \sin(\theta/2)\cos(n\theta)\cos(m\theta)\,d\theta, \quad 0 \leqslant n \leqslant N. \tag{44}$$

In the case of $t_0 = t_1 = \cdots = t_N = 0$, eqns (43) reduce to eqns (23) with $b_m^* = b_m$, since only $q_n^N$ survive on the right-hand side of eqns (43) and their value is $-1$ for $0 \leqslant n \leqslant N$ (all overloads in the cluster are negative after time $t_N$, as all $N$ fiber pairs have been broken). The solution for the axial load in the fibers and the shear stress in the matrix is given by

$$p_n(x,t) = 1 + \sum_{m=0}^{N}\sum_{i=0}^{N} c_{mi}^{-1}[q_i^0 H(t-t_0)\hat{h}(x,t-t_0,n,m) + (q_i^1 - q_i^0)H(t-t_1) \cdot \hat{h}(x,t-t_1,n,m) + \cdots + (q_i^N - q_i^{N-1})H(t-t_N)\hat{h}(x,t-t_N,n,m)] \tag{45}$$

$$\tau_n(x,t) = -\sum_{m=0}^{N}\sum_{i=0}^{N} c_{mi}^{-1}[q_i^0 H(t-t_0)\hat{g}(x,t-t_0,n,m) + (q_i^1 - q_i^0)H(t-t_1) \cdot \hat{g}(x,t-t_1,n,m) + \cdots + (q_i^N - q_i^{N-1})H(t-t_N)\hat{g}(x,t-t_N,n,m)] \tag{46}$$

where the functions $\hat{h}$ and $\hat{g}$ are defined by

$$\hat{h}(x,t-t_i,n,m) \equiv \int_0^\pi h(x,t-t_i,\theta)\cos(m\theta)\cos(n\theta)\sin(\theta/2)\,d\theta \tag{47}$$

$$\hat{g}(x,t-t_i,n,m) \equiv \int_0^\pi g(x,t-t_i,\theta)\cos(m\theta)[\cos(n\theta) - \cos((n-1)\theta)]\,d\theta \tag{48}$$

where $h(x,t,\theta)$ and $g(x,t,\theta)$ are given in Appendix A for the power-law creep compliance model.

Even though the above solution is different from the case of simultaneous breaks for time $t \cong t_N$, the large time behavior ($t \gg t_N$) is the same as if all breaks had occurred simultaneously. To see this assume that $t_m$, $0 \leqslant m \leqslant N$, are all of $O(1)$ and examine the behavior of eqns (47) and (48) as $t \to \infty$. As can be shown by considering the asymptotic expansion of the solution for the fiber loads (eqns (38)), $\hat{h}(x,t-t_i,n,m)$ and $\hat{h}(x,t-t_j,n,m)$ differ from each other by terms of $O[(t_j-t_i)/t^{1+n/2}]$ for $0 \leqslant i,j \leqslant n$. Similar arguments hold for $\hat{g}(x,t-t_i,n,m)$ as well. Neglecting these terms, eqns (45) and (46) reduce to

$$p_n(x,t) = 1 + \sum_{m=0}^{N}\sum_{i=0}^{N} c_{mi}^{-1} q_i^N \hat{h}(x,t,n,m), \quad t \to \infty \tag{49}$$

$$\tau_n(x,t) = -\sum_{m=0}^{N}\sum_{i=0}^{N} c_{mi}^{-1} q_i^N \hat{g}(x,t,n,m), \quad t \to \infty. \tag{50}$$

Noting that $\sum_{i=0}^{N} c_{mi}^{-1} q_i^N = -b_m$, we recover the results for the simultaneous breaks given by eqns (35) and (36). This implies that small delays in the breaking of fibers will not affect the overload profiles of the intact fibers after a large time has elapsed (fading memory matrix material).

## 6. THE SHEAR-LAG FORMULATION FOR RELAXATION EXPERIMENTS

The shear-lag problem has been formulated primarily to explain the way in which the intact fibers are overloaded whenever breaks occur. The boundary conditions therefore are dictated by the fact that broken fibers cannot carry any load. A different phenomenon takes place, however, when a relaxation experiment is performed. A possible model for such an experiment (to be also called an indentation experiment) for a unidirectional composite is

to assume that there are no tensile tractions in one end (i.e. $P_z = 0$ at $X \to \infty$), while the fibers on the other end are clamped (i.e. $U_n = 0$ at $X = 0$), except for a number of them on which non-zero displacements are imposed.

If we assume for the time being that $P_z$ is not zero, the only difference from the formulation of Section 2 is boundary conditions (8b), which now become

$$u_n = u_n^0 \equiv U_n^0 \sqrt{(P_z^2 H / G_c A E B)}, \quad |n| \leqslant N, \quad x = 0, \quad t > 0. \tag{51}$$

Going exactly through the same steps as in the first section we end up having to solve an algebraic system for the determination of the unknown coefficients $a_m$ of the form

$$\sum_{m=0}^{N} a_m \int_0^{\pi} \cos(m\theta) \cos(n\theta)\, d\theta = u_n^0, \quad 0 \leqslant n \leqslant N. \tag{52}$$

The results for the axial fiber loads are

$$p_n(x,t) = 1 - 2 \sum_{m=0}^{N} a_m \int_0^{\pi} L^{-1}\{\exp[-2 \sin(\theta/2)\sqrt{(s\bar{\mathcal{G}}(s))}x]\sqrt{(s\bar{\mathcal{G}}(s))}/s\} \cdot \sin(\theta/2) \cos(m\theta) \cos(n\theta)\, d\theta \tag{53}$$

and for the power-law creep compliance model introduced in Section 3 they are given by

$$p_n(x,t) = 1 - 4 \sum_{m=0}^{N} a_m \int_0^{\pi} g(x,t,\theta) \sin(\theta/2) \cos(m\theta) \cos(n\theta)\, d\theta \tag{54}$$

where $g(x,t,\theta)$ is given in Appendix A. The load $p_n$ is plotted in Fig. 9, for the case of one

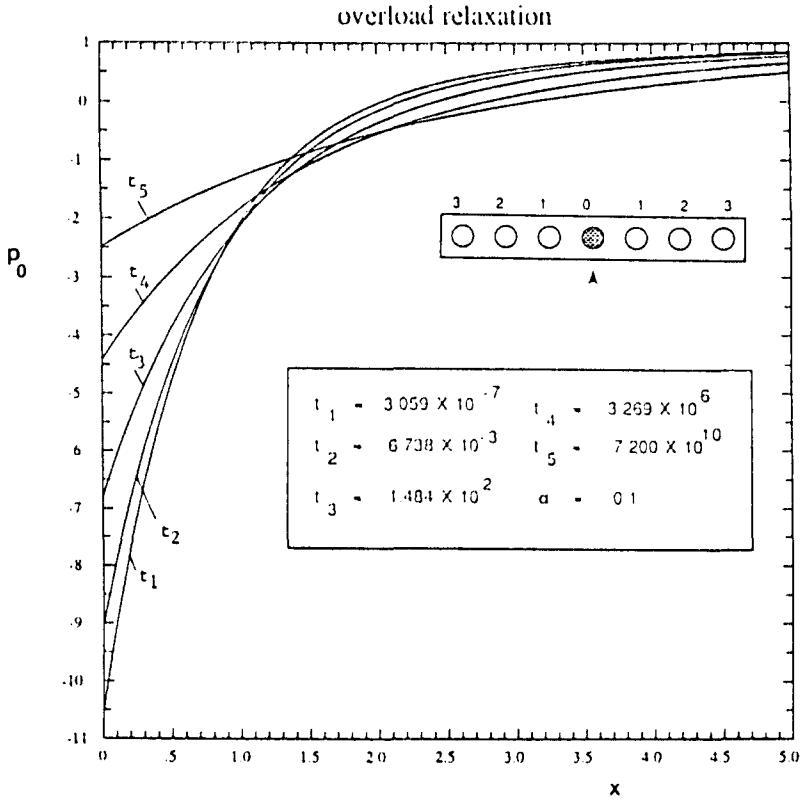


Fig. 9(a). Load of the displaced fiber for various times.

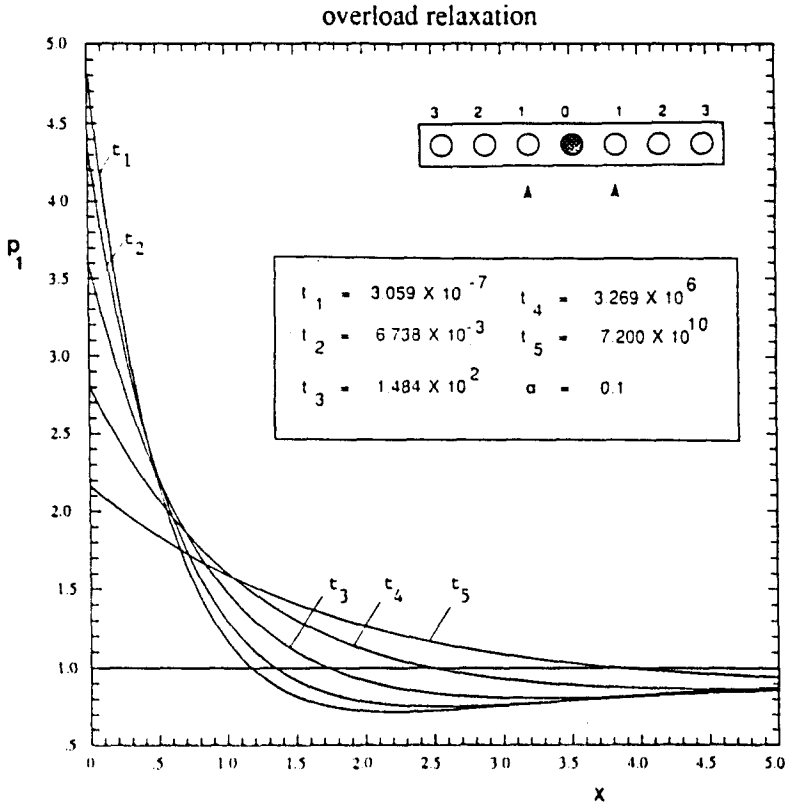


Fig. 9(b). Load of the fiber next to the displaced fiber for various times.

indented fiber with $u_0^0 = 10$, for the displaced and its adjacent fibers ($\alpha = 0.1$). The overload relaxation in the intact fiber is evident as the indented fiber relaxes its compressive load with increasing time. The asymptotic expansion of eqn (54) as $t \to \infty$ is given by

$$p_n(x,t) \cong 1 - 2[\Gamma(1-\alpha/2)]^{-1}[\Gamma(1+\alpha)]^{-1/2}\frac{1}{t^{\alpha/2}}\sum_{m=0}^{N} a_m \int_0^{\pi} \cos(m\theta)\cos(n\theta)\sin(\theta/2)\,d\theta$$

$$+4\frac{\sin(\alpha\pi)}{\alpha\pi}\frac{x}{t^{\alpha}}\sum_{m=0}^{N} a_m \int_0^{\pi} \cos(m\theta)\cos(n\theta)\sin^2(\theta/2)\,d\theta. \quad (55)$$

Note that for $x = 0$ the third term on the right-hand side of eqn (55) vanishes and the load in the fibers relaxes as $t^{-\alpha/2}$.

If the applied $P_\infty$ is zero, then a different nondimensionalization scheme is necessary for $u_n$ and $p_n$. By selecting the imposed $U_0^0$ as a reference length, eqn (51) is replaced by

$$u_n = u_n^0 = U_n^0/U_0^0, \quad |n| \leqslant N, \quad x = 0, \quad t > 0 \quad (56)$$

while the load $p_n$ is given by eqn (54) if $p_n$ is replaced by $(p_n + 1)$, and with the following normalization for the load:

$$p_n = P_n/U_0^0\sqrt{(G_c AEB/H)}. \quad (57)$$

The result is then eqn (54) or eqn (55) with unity omitted and $a_m$ obtained by solving eqn (52). The curves for $p_n$ vs $x$ look like those in Figs 9(a) and (b), except that the $p_n$-axis is shifted vertically so that the zero of the new axis corresponds to one of the old axis. Since there is only one indented fiber in Figs 9(a) and (b), the displacement of that fiber $U_0^0$ at

$x = 0$ does not enter into the results of Figs 9(a) and (b), as it is used for the non-dimensionalization scheme.

## 7. CONCLUSIONS

The viscoelastic constitutive behavior in shear of the matrix material has the following implications in the time behavior of the stress fields near breaks in a unidirectional composite under tension.

(1) The overload region in the intact fibers grows with time and it grows in a self-similar way for large times.

(2) The effective load transfer length grows as $t^{\alpha/2}$ for large times, where $\alpha$ is the exponent of time in the power-law creep compliance function for the matrix.

(3) The applied loads in an indentation experiment relax like $t^{-\alpha/2}$ for large times.

*Acknowledgements*—The authors would like to express their gratitude to the reviewer for his useful suggestions, especially on revising Section 5. This work was partly supported by the U.S. Army Research Office through the MSI of Cornell University.

## REFERENCES

Carrier, G. F., Krook, M. and Pearson, C. E. (1966). *Functions of a Complex Variable*. McGraw-Hill, New York.
Christensen, R. M. (1982). *Theory of Viscoelasticity*. Academic Press, New York.
Churchill, R. V. (1972). *Operational Mathematics*, 2nd Edn. McGraw-Hill, Tokyo.
Eringen, A. C. and Kim, B. S. (1974). Stress concentration in filamentary composites with broken fibers. *Lett. Appl. Engng Sci.* **2**, 69–89.
Fichter, W. B. (1969) Stress concentration around broken filaments in a filament-stiffened sheet. NASA TN D-5453, Langley Research Center.
Fichter, W. B. (1970). Stress concentrations in filament-stiffened sheets of finite length. NASA TN D-5947, Langley Research Center.
Goree, J. G. and Gross, R. S. (1979). Analysis of a unidirectional composite containing broken fibers and matrix damage. *Engng Fract. Mech.* **13**, 563–578.
Goree, J. G. and Gross, R. S. (1980). Stresses in a three-dimensional unidirectional composite containing broken fibers. *Engng Fract. Mech.* **13**, 395–405.
Hedgepeth, J. (1961). Stress concentrations in filamentary structures. NASA TN D-882, Langley Research Center.
Hedgepeth, J. and Van Dyke P. (1967). Local stress concentrations in imperfect filamentary composite materials. *J. Composite Mater.* **1**, 294–309.
Lifshitz, J. M. and Rotem, A. (1970) Time-dependent longitudinal strength of unidirectional fibrous composites. *Fibre Sci. Technol.* **3**, 1–20.
Phoenix, S. L., Schwartz, P. and Robinson, H. H., IV (1988). Statistics for the strength and lifetime in creep-rupture of model carbon/epoxy composites. *Composites Sci. Technol.* **32**, 81–120.
Pomeroy, C. D. (Editor) (1978). Creep of engineering materials. *J. Strain Analysis Monograph, I. Mech. E.*
Reedy, E. D. Jr. (1984) Fiber stresses in a cracked monolayer: comparison of shear-lag and 3-D finite element predictions. *J. Composite Mater.* **18**, 595–607.
Schapery, R. A. (1962) Approximate methods of transform inversion for viscoelastic stress analysis. *Proc. 4th U.S. Natl Congr. Appl. Mech., ASME*, pp. 1075–1085.
Schapery, R. A. (1967). Stress analysis of viscoelastic composite materials. *J. Composite Mater.* **1**, 228–267.
Van Dyke, P. and Hedgepeth, J. M. (1969). Stress concentrations from single-filament failures in composite materials. *Text. Res. J.* **39**, 618–626.

## APPENDIX A

For the inversion of the Laplace transforms reported in eqns (29) and (30) a contour has been selected around zero and the negative real axis on the complex plain. Contour integration yields the functions $h(x, t, 0)$ and $g(x, t, 0)$, which are given by

$$h(x,t,0) = 1 - \frac{1}{\pi}\int_0^\infty \exp(-tr)\exp\left[-\lambda\sqrt{\left(\frac{r'}{\rho}\right)}\cos\left(\frac{\alpha\pi-\varphi}{2}\right)\right]\sin\left[\lambda\sqrt{\left(\frac{r'}{\rho}\right)}\sin\left(\frac{\alpha\pi-\varphi}{2}\right)\right]\frac{dr}{r} \quad (A1)$$

$$g(x,t,0) = -\frac{1}{2\pi}\int_0^\infty \exp(-tr)\exp\left[-\lambda\sqrt{\left(\frac{r'}{\rho}\right)}\cos\left(\frac{\alpha\pi-\varphi}{2}\right)\right]\sin\left[\lambda\sqrt{\left(\frac{r'}{\rho}\right)}\sin\left(\frac{\alpha\pi-\varphi}{2}\right) - \left(\frac{\alpha\pi-\varphi}{2}\right)\right]\sqrt{\left(\frac{r'}{\rho}\right)}\frac{dr}{r}. \quad (A2)$$

The quantities $\lambda$, $\rho$ and $\varphi$ have the following evaluations:

$$\lambda = 2 \sin (\theta/2) x \tag{A3}$$

$$\rho = \sqrt{\{[r^{\alpha} \cos (\alpha\pi) + \Gamma(\alpha+1)]^2 + [r^{\alpha} \sin (\alpha\pi)]^2\}} \tag{A4}$$

$$\varphi = \tan^{-1}\left[\frac{r^{\alpha} \sin (\alpha\pi)}{r^{\alpha} \cos (\alpha\pi) + \Gamma(\alpha+1)}\right], \quad 0 < \varphi < \pi. \tag{A5}$$

## APPENDIX B

Suppose we want to find the function $\varphi(t)$, if its Laplace transform $\bar{\varphi}(s)$ is known, namely we have to solve the integral equation

$$\bar{\varphi}(s) = \int_0^{\infty} \exp(-s\eta)\varphi(\eta)\, d\eta. \tag{B1}$$

If we take the $k$th derivative of eqn (B1) with respect to $s$ and evaluate it at $s = (k+c)/t$, we get the following result:

$$\left.\frac{d^k \bar{\varphi}}{ds^k}\right|_{s=(k+c)/t} = (-1)^k \int_0^{\infty} \eta^k \exp\left[-\frac{\eta(k+c)}{t}\right]\varphi(\eta)\, d\eta. \tag{B2}$$

By making the change of variables $\eta = \exp(v)$, $t = \exp(u)$, $\eta/t = \exp(v-u) = \exp(w)$ the above equation reduces to

$$\frac{(-1)^k (k+c)^{k+1}}{k!\, t^{k+1}}\left(\frac{d^k \bar{\varphi}}{ds^k}\right)\Bigg|_{s=(k+c)/t} = \int_{-\infty}^{\infty} \frac{(k+c)^{k+1}}{k!} \exp[(k+1)w] \exp[-(k+c)\exp(w)]\hat{\varphi}(w+u)\, dw \tag{B3}$$

where $\hat{\varphi}(w+u) = \varphi[\exp(u+w)]$. If we define

$$\delta_k(w) = \frac{(k+c)^{k+1}}{k!} \exp[(k+1)w] \exp[-(k+c)\exp(w)]$$

we can prove that $\delta_k(w) \to \delta(w)$ as $k \to \infty$, where $\delta(w)$ is the Dirac delta function. The left-hand side of eqn (B3) therefore becomes the function $\hat{\varphi}(u) = \varphi(t)$ in the case that $k \to \infty$, that is

$$\varphi(t) = \frac{(-1)^k (k+c)^{k+1}}{k!\, t^{k+1}}\left(\frac{d^k \bar{\varphi}}{ds^k}\right)\Bigg|_{s=(k+c)/t}, \quad k \to \infty. \tag{B4}$$

Suppose that $\hat{\varphi}(w+u)$ can be expanded in a Taylor series about the point $w_0$, namely

$$\hat{\varphi}(w+u) = \hat{\varphi}(w_0+u) + \left.\frac{d\hat{\varphi}}{dv}\right|_{v=w_0+u} (w-w_0) + \cdots \tag{B5}$$

If the first term in the expansion is only retained, the following result is obtained after substitution of eqn (B5) into eqn (B3), for any finite value of $k$:

$$\varphi(t) = \frac{(-1)^k}{k!}\left(s^{k+1}\frac{d^k \bar{\varphi}}{ds^k}\right)\Bigg|_{s=(k+c)\exp(w_0)/t}. \tag{B6}$$

We can improve the above approximation if we substitute eqn (B5) into eqn (B3) and require the vanishing of the integral that corresponds to the second term in the expansion of $\hat{\varphi}(w+u)$ given by eqn (B5), that is

$$\int_{-\infty}^{\infty} \frac{(k+c)^{k+1}}{k!} \exp[(k+1)w] \exp[-(k+c)\exp(w)] \left.\frac{d\hat{\varphi}}{dv}\right|_{v=w_0+u} (w-w_0)\, dw = 0. \tag{B7}$$

The evaluation for $w_0$ that is derived from eqn (B7) is given by

$$w_0 = \int_{-\infty}^{\infty} \frac{(k+c)^{k+1}}{k!} \exp[(k+1)w] \exp[-(k+c)\exp(w)] w\, dw. \tag{B8}$$

In accordance with Schapery's approximation we select $k = 0$. We then calculate from eqn (B8) that $w_0 = -\gamma - \ln(c)$, where $\gamma$ is Euler's constant. We are still left with the freedom to choose $c$, and one idea would be to improve the accuracy of eqn (B6) by requiring the vanishing of the second moment resulting from the second-order terms in the expansion of $\hat{\varphi}(w+u)$, a condition that would fix $c$. We avoid this here however and we select $c = \exp(-\gamma)$ so that $w_0$ becomes zero, with eqn (B6) reducing to

$$\varphi(t) = [s\tilde{\varphi}(s)]|_{s=1/(1-\nu)t}. \tag{B9}$$

Another selection of $c$ implied by the long time asymptotic behavior of $\varphi(t)$ is given in Section 4.

## APPENDIX C

The functions $d_1(n), \ldots, d_5(n)$ appearing in eqn (38) for the expression of the asymptotic behavior of the loads $p_n$ along the fibers have the following explicit evaluations:

$$d_1(n) = \sum_{m=0}^{N} b_m \int_0^{\pi} \cos(m\theta) \cos(n\theta) \sin(\theta/2)\, d\theta$$

$$d_2(n) = 2[\Gamma(1-\alpha/2)]^{-1}[\Gamma(1+\alpha)]^{-1/2} \sum_{m=0}^{N} b_m \int_0^{\pi} \cos(m\theta) \cos(n\theta) \sin^2(\theta/2)\, d\theta$$

$$d_3(n) = \frac{2\sin(\alpha\pi)}{\alpha\pi} \sum_{m=0}^{N} b_m \int_0^{\pi} \cos(m\theta) \cos(n\theta) \sin^3(\theta/2)\, d\theta$$

$$d_4(n) = \frac{4\Gamma(3\alpha/2)}{\pi[\Gamma(1+\alpha)]^{1/2}} \sin(\alpha\pi/2)[\cos^2(\alpha\pi/2) - \tfrac{1}{3}\sin^2(\alpha\pi/2)] \sum_{m=0}^{N} b_m \int_0^{\pi} \cos(m\theta) \cos(n\theta) \sin^4(\theta/2)\, d\theta$$

$$d_5(n) = [\Gamma(1-3\alpha/2)]^{-1}[\Gamma(1+\alpha)]^{-3/2} \sum_{m=0}^{N} b_m \int_0^{\pi} \cos(m\theta) \cos(n\theta) \sin^5(\theta/2)\, d\theta.$$